

Copper and Copper Alloys: Metallographic Techniques and Microstructures

Revised by R.E. Ricksecker, Chase Brass and Copper Co. (retired) and T.F. Bower, Chase Brass and Copper Co.

[<Previous section in this article](#)

Atlas of Microstructures for Copper and Copper Alloys

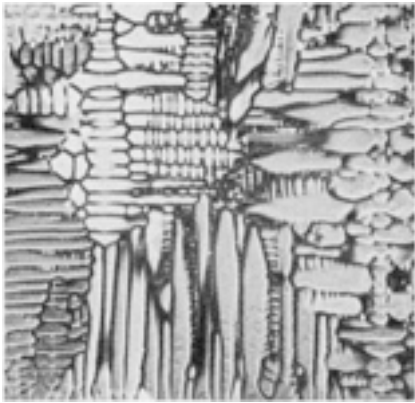


Fig. 1 Alloy 11000 (ETP copper), static cast. Excellent definition of dendritic structure. Etchant 10, [Table 3](#). 5x. (J. Bartholomew)

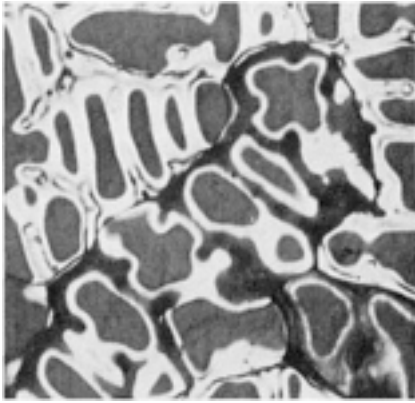


Fig. 2 Same material as [Fig. 1](#), but at higher magnification to show detail of dendritic structure. Etchant 4, [Table 3](#). 75x. (J. Bartholomew)



Fig. 3 Same material as [Fig. 1](#), static cast. Grains from the chilled bottom grew through the dendrite "skeletons," producing a mixed grain structure, Etchant 10, [Table 3](#). 3x

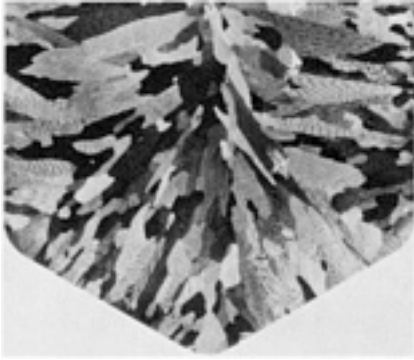


Fig. 4 Alloy 12200 (DHP copper). Longitudinal section of static-cast ingot showing columnar structure. Pouring direction was from top to bottom. Etchant 10, [Table 3](#). 2×. (J. Dibee)

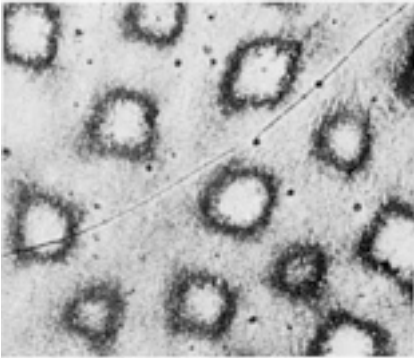


Fig. 5 Same alloy as [Fig. 4](#). Transverse section shows the cross section of the columnar structure and a grain boundary. Etchant 4, then etchant 1, [Table 3](#). 50×. (J. Dibee)

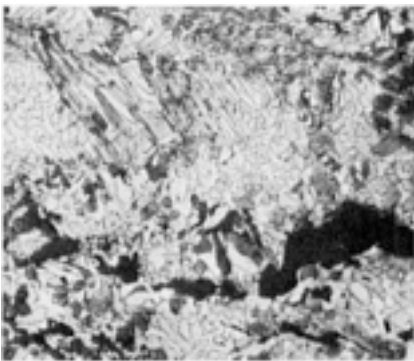


Fig. 6 Alloy 36000 (free-cutting brass), as-cast. Solid-state transformation makes this structure appear unlike an as-cast structure. Etchant 1, [Table 3](#). 50×. (J. Bartholomew)



Fig. 7 Same material as [Fig. 6](#), with primary dendrites of α phase darkened. Lead appears as small spheroids. Etchant 1, [Table 3](#). 50×. (J. Dibee)

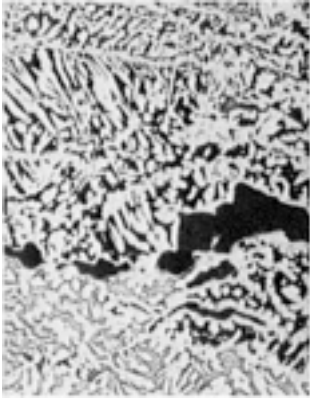


Fig. 8 Same alloy as [Fig. 6](#), with β phase darkened by preferential attack of the etchant. In this case, α phase is formed in the solid state during cooling. Etchant 16, [Table 3](#). 50 \times . (J. Dibee)



Fig. 9

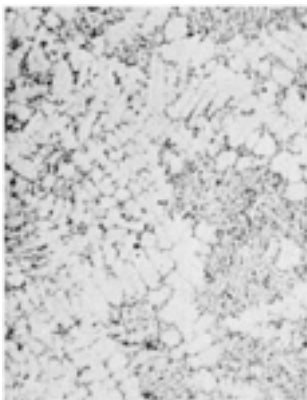


Fig. 10

Same alloy as [Fig. 6](#), semicontinuous cast. [Fig. 9](#): α -phase dendrites in the columnar zone near the outside edge of the ingot. [Fig. 10](#): mixed α - and β -phase dendrites near the center of the ingot. Etchant 1, [Table 3](#) 30 \times . ([Ref 1](#))

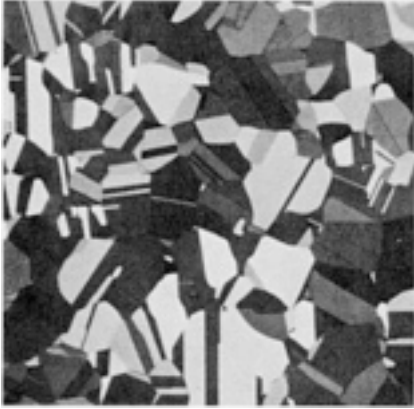


Fig. 11 Alloy 26000 (cartridge brass), annealed. Polarized light illumination was used to increase contrast of the microstructure. Etchant 18, then etchant 19, [Table 3](#). 55 \times . (J. Dibee)

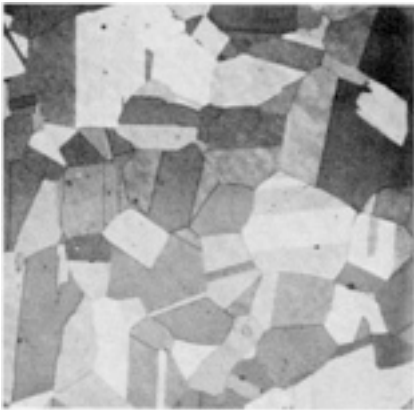


Fig. 12 Alloy 68700 (arsenical aluminum brass), annealed. Structure is α -brass, with the aluminum in solid solution. Etchant 18, [Table 3](#). 55 \times . (J. Dibee)

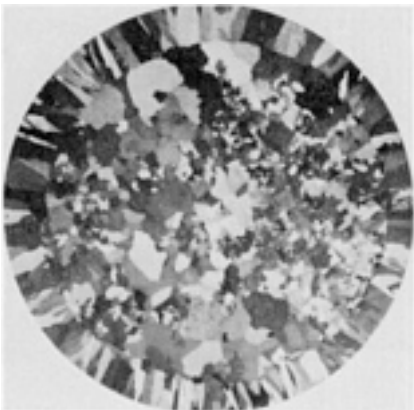


Fig. 13 Alloy 46400 (uninhibited naval brass), as-cast. Transverse macrosection showing the columnar structure of the outer edges of the casting that result from more rapid cooling near the surface of the casting. Etchant 12, [Table 3](#). 1.5 \times . (J. Dibee)

[graphic]

Fig. 14 Same specimen as [Fig. 13](#), except at higher magnification to reveal dendritic microstructure. Etchant 1, then etchant 16, [Table 3](#). 30×. (J. Dibee)

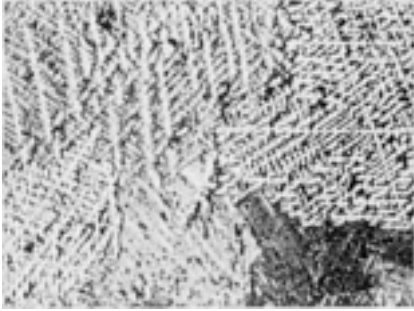


Fig. 15 Alloy 68700 (arsenical aluminum brass), as-cast. Macrosection showing typical dendritic structure, See [Fig. 16](#) for detail. Etchant 18, then etchant 16, [Table 3](#). 4×. (J. Dibee)



Fig. 16 Same as [Fig. 15](#), except at higher magnification to reveal more detail of the structure. Same etchants as [Fig. 15](#). 75×. (J. Dibee)

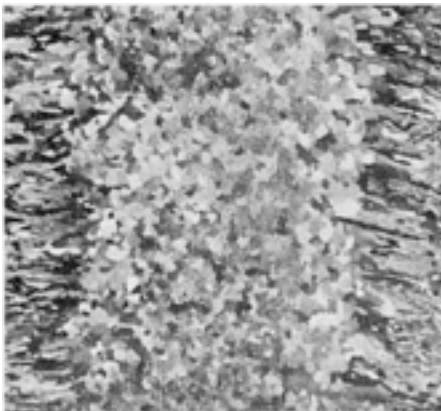


Fig. 17 Alloy 71500 (copper nickel, 30% Ni), as-cast. Longitudinal section showing columnar structure near the surface of the billet. The grains are inclined upward from horizontal by up to 30° due to convection in the initial state of freezing. Etchant 18, then etchant 16, [Table 3](#). 0.3×. (J. Bartholomew)

[graphic]

Fig. 18 Alloy 26000 (cartridge brass), cast, slowly cooled, and quenched. Primary dendrites aligned in $\langle 100 \rangle$ crystallographic directions. The fine, quenched structure has the same orientation as the coarse dendrites. Etchant 1, [Table 3](#), then electropolished with electrolyte 1, [Table 2](#). 30 \times . (J. Dibee)



Fig. 19 Same alloy and processing as [Fig. 18](#). Higher magnification shows that fine dendrites originate in the coarse ones and have the same orientation. Dendrites starting in directions that are not $\langle 100 \rangle$ do not grow very far. Same etchant and electrolyte as [Fig. 18](#). 85 \times . (J. Dibee)

[graphic]

Fig. 20 Alloy 70600 (copper-nickel, 10% Ni), semicontinuous cast. Microstructure shows the distinct segregation of the copper-rich phase (dark) and the nickel-rich phase (light). Etchant 17, [Table 3](#). 50 \times . (J. Dibee)

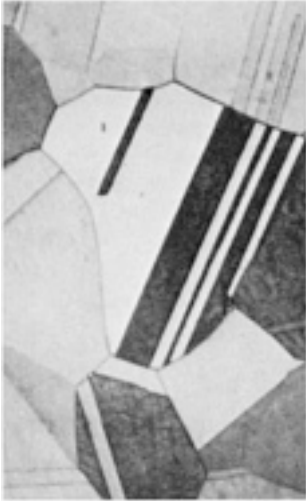


Fig. 21 Alloy 46400 (uninhibited naval brass), extruded, drawn, and annealed. Structure shows twinned grains resulting from annealing. Etchant 16, [Table 3](#). 300×. (J. Dibee)

[graphic]

Fig. 22 Alloy 18200 (chromium copper, 0.8% Cr), solutionized 5 min at 1010 °C (1850 °F). Solutionizing increases solubility of chromium, which gives higher hardness after quenching and aging. However, if all chromium goes into solid solution, uncontrolled grain growth results, starting where there is the most cold work before heat treatment (right). Excessive grain growth embrittles grain boundaries; temperature, chromium content, cold work, and time at temperature must be controlled to prevent complete solution of chromium and uncontrolled grain growth. 0.45×. (T. Cobb)

[graphic]

Fig. 23

[graphic]

Fig. 24

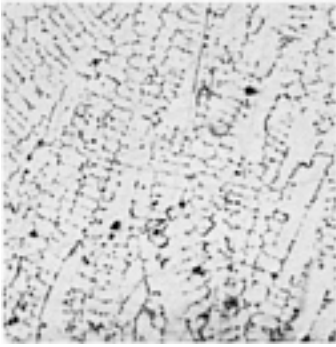


Fig. 25



Fig. 26

The effect of oxygen content on the microstructure of as-cast, copper-oxygen alloys. Oxygen contents less than 0.39% result in primary dendrites of copper (light) plus eutectic (mottled areas of small, round oxide in copper). [Fig. 23](#): 0.024% O. [Fig. 24](#): 0.05% O. [Fig. 25](#): 0.09% O. [Fig. 26](#): 0.18% O. As-polished. 100×

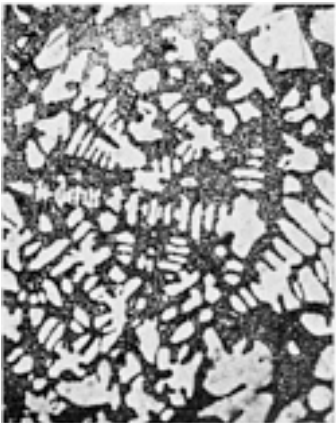


Fig. 27

[graphic]

Fig. 28

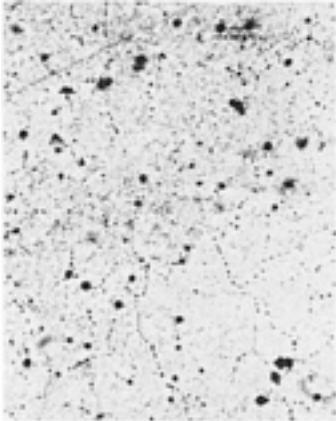


Fig. 29

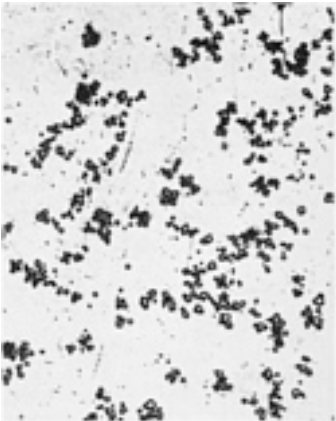


Fig. 30

Same as [Fig. 23](#), [24](#), [25](#), and [26](#). [Fig. 27](#): 0.23% O. [Fig. 28](#): 0.32% O. [Figures 29](#) and [30](#), containing more than 0.39% O, have structures consisting of particles or dendrites of oxide (dark) and eutectic. [Fig. 29](#): 0.44% O. [Fig. 30](#): 0.50% O. As-polished. 100×

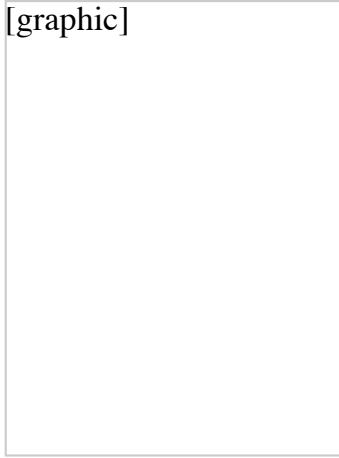


Fig. 31

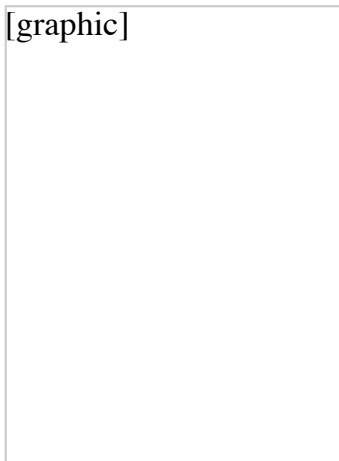


Fig. 32



Fig. 33

[graphic]

Fig. 34

Same as [Fig. 23](#), [24](#), [25](#), and [26](#), with dark oxide dendrites in a eutectic matrix. [Fig. 31](#): 0.60% O. [Fig. 32](#): 0.70% O. [Fig. 33](#): 0.78% O. [Fig. 34](#): 0.91% O. As-polished. 100×

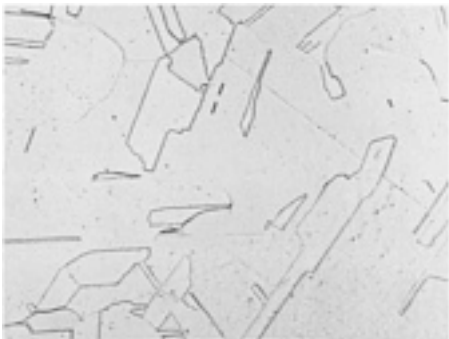


Fig. 35 Copper 10200 (OF copper), hot-rolled bar. Large, equiaxed, twinned grains. Etchant 1, [Table 3](#). 100×



Fig. 36 Same as [Fig. 35](#), cold worked, annealed 30 min at 850 °C (1560 °F). Equiaxed, recrystallized grains, containing twinned areas. Etchant 4, [Table 3](#). 250×

[graphic]

Fig. 37 Same as [Fig. 35](#), hot-rolled bar, heated 1 h in air to 665 °C (1225 °F). Specimen from near

surface shows Cu_2O (dark dots) caused by oxygen penetration during heating. Etchant 1, [Table 3](#). 250×

[graphic]

Fig. 38 Copper 11000 (ETP copper) hot-rolled rod. Transverse section shows equiaxed grains and dispersion of Cu_2O particles. Etchant 4, [Table 3](#). 250×

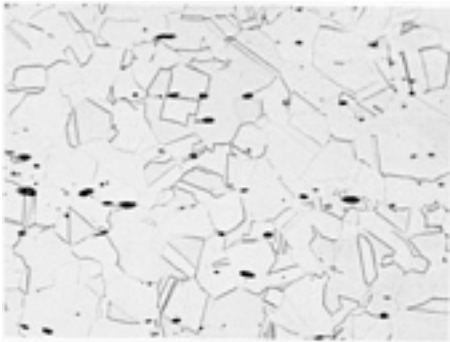


Fig. 39 Same as [Fig. 38](#). Longitudinal section shows equiaxed grains and well-dispersed, slightly elongated Cu_2O particles (dark dots). Etchant 4, [Table 3](#). 250×

[graphic]

Fig. 40 Same as [Fig. 38](#), extruded rod. Longitudinal section showing equiaxed grains and dispersed Cu_2O (dark dots). Etchant 4, [Table 3](#). 400×

[graphic]

Fig. 41 Same as [Fig. 38](#), heated in hydrogen. Hydrogen diffused into the copper, reacted with Cu_2O at the grain boundaries, formed steam, and forced the copper grains apart, causing embrittlement

and porosity. See also [Fig. 42](#). Etchant 4, [Table 3](#). 75×



Fig. 42 Same as [Fig. 38](#), heated to 850 °C (1560 °F) in an atmosphere containing hydrogen. Structure shows same voids as [Fig. 41](#). Etchant 4, [Table 3](#). 250×



Fig. 43 Copper 12500 (FRTP copper) hot-rolled strip 12.7 mm (0.5 in.) thick. Structure consists of twinned grains of copper, with stringers of Cu_2O particles resulting from segregation of the oxide in the ingot during casting. Etchant 1, [Table 3](#). 200×

[graphic]

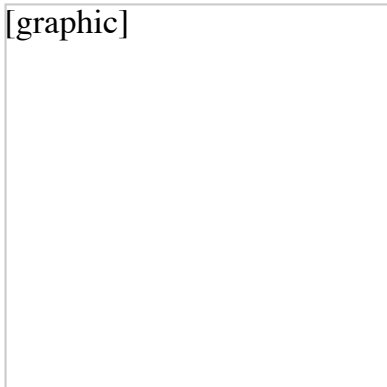


Fig. 44 Copper 12200 (DHP copper). Internal oxidation (presence of dark dots of P_2O_5). Etchant 4, [Table 3](#). 75×

[graphic]

Fig. 45 Same metal as [Fig. 44](#). Lap defect in the fin of a condenser tube. Lap was caused by tool misalignment during the rolling of fins on the tube. Etchant 4, [Table 3](#). 75×

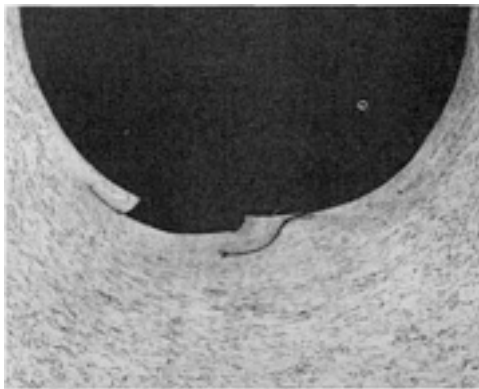


Fig. 46 Same as [Fig. 45](#). Lap defect between fins of a condenser tube, caused by tool misalignment during fin rolling. Etchant 4, [Table 3](#). 75×

[graphic]

Fig. 47 Copper 14520 (DPTE copper) hot-rolled and drawn rod. Dark particles elongated in the rolling direction are copper telluride, which improves machinability. Etchant 7, [Table 1](#). 250×

[graphic]

Fig. 48 Copper 14700 (sulfur-bearing copper) rod, cold worked to 50% reduction. Transverse section shows dispersion of round particles of Cu₃S, which improves machinability. Etchant 7, [Table 1](#). 200×

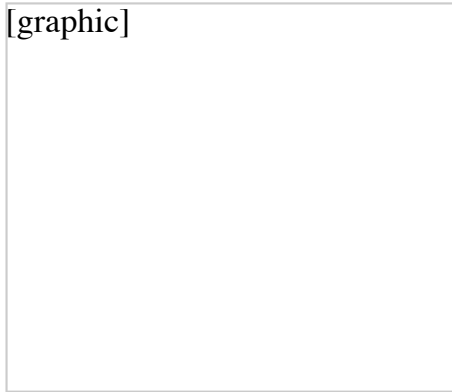


Fig. 49 Alloy 17200 (beryllium copper), solution treated 10 min at 790 °C (1450 °F) and water quenched. Typical hardness is 62 HRB. Structure is equiaxed grains of super-saturated solid solution of beryllium in copper. Etchant 3, [Table 3](#). 300×

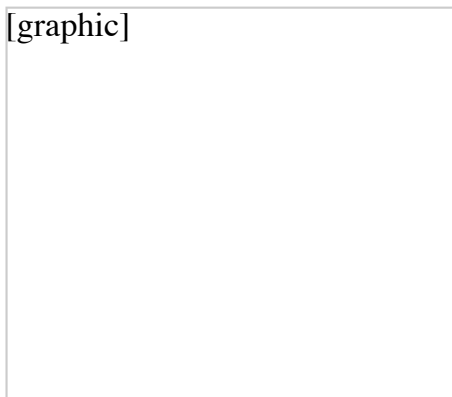


Fig. 50 Same alloy and processing as [Fig. 49](#), but aged 3 h at 360 °C (600 °F) after solution treatment. Typical hardness is 37 HRC. Copper-beryllium precipitate at grain boundaries and within a grains. Etchant 3, [Table 3](#). 300×

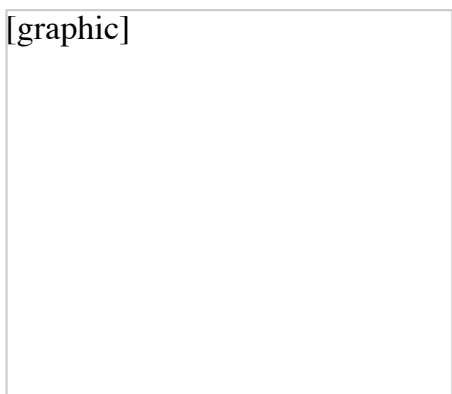


Fig. 51 Same alloy and processing as [Fig. 49](#), except reduced 11% by cold rolling to quarter-hard temper. Typical hardness is 79 HRB. Alpha grains are elongated in the direction of rolling. Etchant 3, [Table 3](#). 300×

[graphic]

A large rectangular area that is currently blank, representing a micrograph of a copper weld joint.

Fig. 52 Copper 11000 (ETP copper) cold-rolled bar, annealed approximately 1 h by holding at 375 °C (705 °F), then tungsten arc welded in two passes using straight-polarity direct current and copper 11000 filler metal. See [Fig. 53](#) for structure details at the fusion zone edge. Etchant 1, [Table 3](#). 2×

[graphic]

A large rectangular area that is currently blank, representing a micrograph of the edge of a fusion zone.

Fig. 53 Edge of fusion zone of weld in [Fig. 52](#). Gas porosity (dark areas) in fusion zone (upper left) and in the heat-affected zone (bottom right). Etchant 1, [Table 3](#). 250×

[graphic]

A large rectangular area that is currently blank, representing a micrograph of copper grains.

Fig. 54 Copper 10100 (OFE copper) bar, electron beam welded without filler metal. Columnar grains in fusion zone (middle) and original equiaxed grains in base metal. The scattered black dots along the edge of the fusion zone are gas porosity. Etchant 2, [Table 3](#). 35×

[graphic]

Fig. 55 Alloy C70600 (copper nickel, 10% Ni), 2.3 mm (0.090 in.) thick. Laser welded to 1020 steel base. Weld made with 2.0 kW of laser input energy at travel speed of 17 to 25.4 mm/s (40 to 60 in./min). No melting of the steel base occurred. Etchant 21, [Table 3](#). 15×. ([Ref 2](#))

[graphic]

Fig. 56 Copper 10100 (OFE copper) brazed with BCuP-5 filler metal. Silver-copper-phosphorus eutectic (mottled gray) in the joint, with large dendrites of copper solid solution (light gray) extending into the joint from the grains of unalloyed base metal. Grains of unalloyed copper in the base metal are medium size. Compare with [Fig. 53](#). Etchant 5, [Table 3](#). 125×

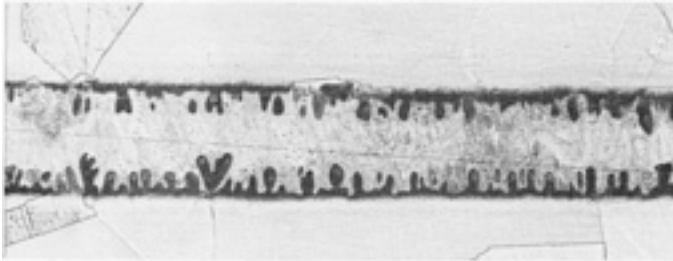


Fig. 57 Same as [Fig. 56](#), brazed with BAg-8a filler metal. Silver-copper eutectic (mottled gray) in the joint, with small dendrites of copper solid solution (dark) extending into the joint from the unalloyed base metal. Grains of unalloyed copper in the base metal are extremely large. Etchant 5, [Table 3](#). 70×

[graphic]



Fig. 58 Same alloy as [Fig. 55](#), except 2.5 mm (0.1 in.) thick. Alloy laser welded to 1020 steel, with a 0.8-mm (0.03-in.) gap between pieces. Laser input energy was 5 kW; travel speed, 17 mm/s (40 in./min). Etchant 21, [Table 3](#). 20×. ([Ref 2](#))

[graphic]



Fig. 59 Brazed joint between tubes of copper 12200 (DHP copper). Filler metal was BAg-1. See [Fig. 61](#) for details of structure. Etchant 4, [Table 3](#). 75×

[graphic]

Fig. 60 Brazed joint between tubes of copper 12200. Filler metal was BCuP-5. See [Fig. 62](#) for details of structure. Etchant 4, [Table 3](#). 100×

[graphic]

Fig. 61 Brazed joint in [Fig. 59](#), except at higher magnification. Filler metal (middle) has copper-rich dendrites in a matrix of silver-copper-zinc-cadmium eutectic (dark gray, mottled). Etchant 4, [Table 3](#). 540×

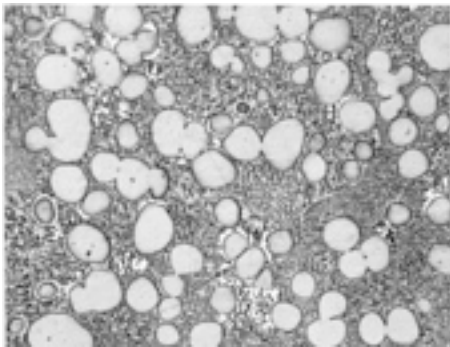


Fig. 62 Brazed joint in [Fig. 60](#), except at a higher magnification. Filler metal (top) has copper-rich dendrites (light gray) in a matrix of silver-copper-phosphorus. Base metal is at the bottom. Etchant 4, [Table 3](#). 540×

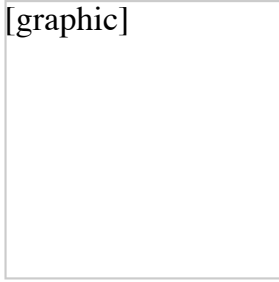


Fig. 63 Alloy 26000 (cartridge brass) drawn cup, showing "orange peel" (rough surface). See [Fig. 65](#) for grain structure. Etchant 1, [Table 3](#). Actual size

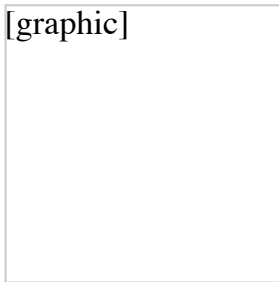


Fig. 64 Same as [Fig. 63](#), with a smooth surface. See [Fig. 66](#) for structural details. Etchant 1, [Table 3](#). Actual size

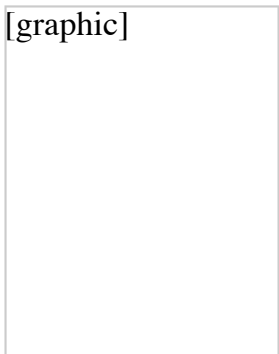


Fig. 65 Grain structure of drawn cup in [Fig. 63](#). The rough surface of the cup was caused by the large grain size. Etchant 1, [Table 3](#). 85×



Fig. 66 Structure of the drawn cup in [Fig. 64](#). Because grains are small, the cup has a smooth surface. Etchant 1, [Table 3](#). 85×

[graphic]



Fig. 67 Copper 12200 drawn condenser tube, with a branched intergranular stress-corrosion crack starting at an outside surface. See [Fig. 68](#) for details of a similar crack. Potassium dichromate. 1100×

[graphic]



Fig. 68 Same material and processing as [Fig. 67](#). An intergranular stress-corrosion crack, possibly caused by amine boiler-treatment compounds in boiler condensate. Potassium dichromate. 500×

[graphic]



Fig. 69 Alloy 26000 (cartridge brass) tube, drawn, annealed and cold-reduced 5%. Typical intergranular stress-corrosion crack, with some branching. $\text{NH}_4\text{OH} + \text{H}_2\text{O}_2$. 150×

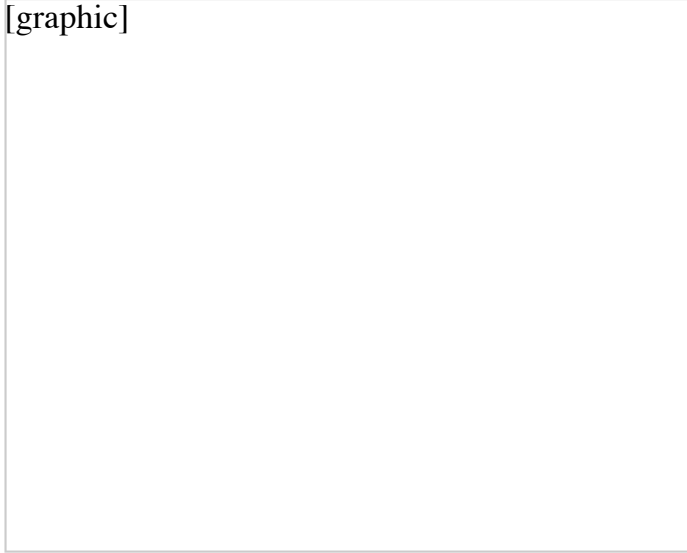


Fig. 70 Alloy 26000 (cartridge brass), showing a transgranular corrosion crack. Note the lack of branching in the inner (fatigue) section of the crack. Etchant 1, [Table 3](#). 130×

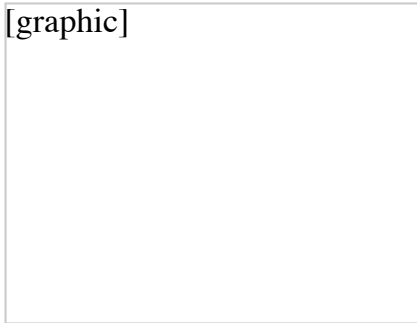


Fig. 71 Copper 11000 (ETP copper) 16-mm (0.625-in.) diam bar, tested at 350 °C (660 °F) at an extension rate of 0.03 mm/s (0.00114 in./s). W-type void formation. Etchant 1, [Table 3](#). 160×

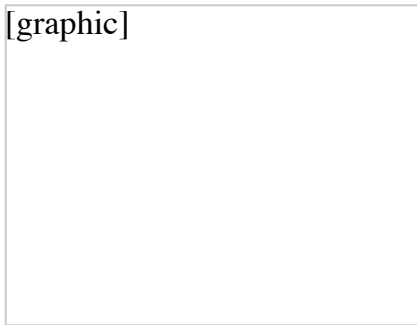


Fig. 72 Same material and processing as [Fig. 71](#). Magnetized view showing a W-type crack. 645×

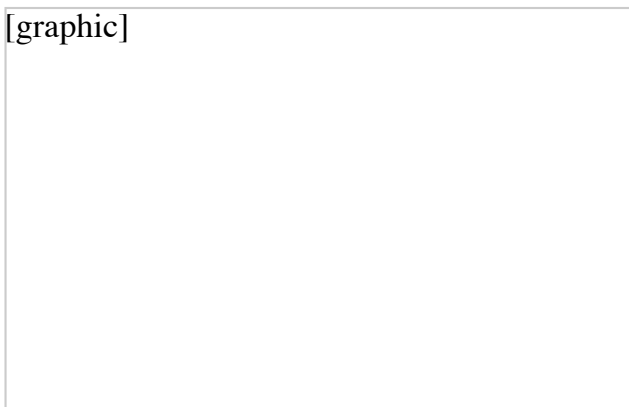


Fig. 73 Copper 10100 (OFE copper) 10-mm (0.375-in.) diam rod, rolled to 1.3-mm (0.052 in.) strip and annealed. Crack formed at the intersection of shearing grain boundary and the surface. The specimen was tested at 550 °C (1020 °F) with an extension rate of 0.03 mm/s (0.001 in./s). Etchant 1, [Table 3](#). 910×

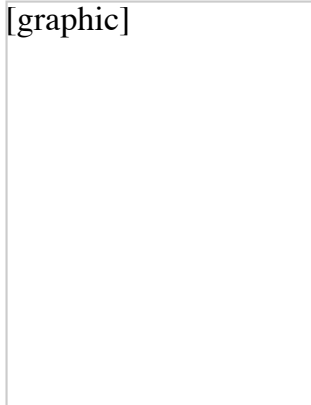


Fig. 74 Same as [Fig. 73](#). A small crack formed at the intersection of a grain boundary and the surface. Same testing conditions and etchant as [Fig. 73](#). 1000×

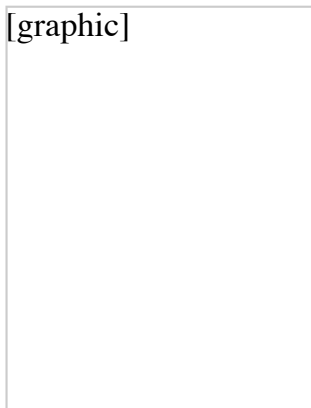


Fig. 75 Copper 10200 (OF copper) 6.3-mm (0.25-in.) diam rod. Microstructure after testing at 550 °C (1020 °F) with an extension rate of 0.03 mm/s (0.001 in./s). Etchant 1, [Table 3](#). 800×



Fig. 76

[graphic]**Fig. 77**

Alloy 26000 (cartridge brass) hot rolled to 10 mm (0.4 in.) thick, annealed to a grain size of 15 μm , cold rolled to 40% to 6 mm (0.24 in.) thick, and annealed to a grain size of 120 μm . Diagram in lower left corner of each micrograph indicates the view relative to the rolling plane of the sheet. Nominal tensile strength of 296 MPa (43,000 psi). Etchant 1, [Table 3](#). 75 \times

[graphic]**Fig. 78**[graphic]**Fig. 79**

Same alloy and processing as [Fig. 76](#) and [77](#), except reduced by cold rolling from 6 mm (0.24 in.) to 4 mm (0.15 in.) thick. Hard temper; nominal tensile strength of 52A MPa (76 000 psi). Etchant 1, [Table 3](#). 75 \times

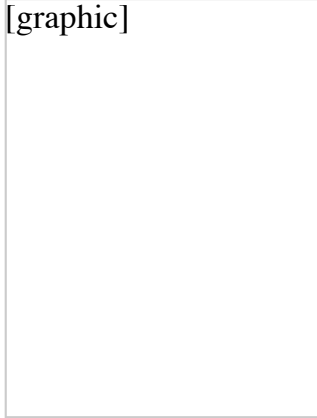


Fig. 80

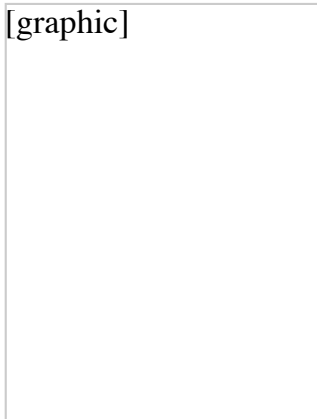


Fig. 81

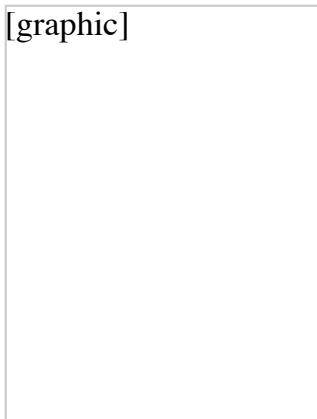


Fig. 82

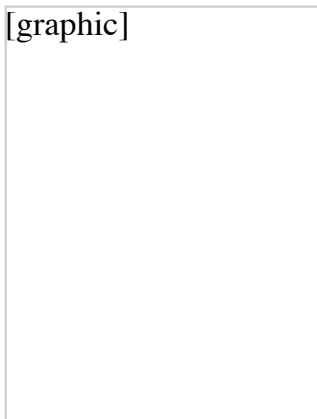


Fig. 83

Alloy 26000 (cartridge brass), processed to obtain various grain sizes. Preliminary processing: hot

rolled, annealed, cold rolled, annealed to a grain size of 25 μm , cold rolled to 70% reduction. Final anneal temperature gives difference in grain sizes. [Fig. 80](#): grain size is 5 μm final annealed at 330 °C (625 °F). [Fig. 81](#): grain size is 10 μm final annealed at 370 °C (700 °F). [Fig. 82](#): grain size is 15 μm ; final annealed at 405 °C (760 °F). [Fig. 83](#): grain size is 20 μm ; final annealed at 425 °C (800 °F). Etchant 1, [Table 3](#). 75 \times

[graphic]

Fig. 84

[graphic]

Fig. 85

[graphic]

Fig. 86



[graphic]

Fig. 87

Same as [Fig. 80](#), [81](#), [82](#), and [83](#). [Fig. 84](#): grain size is 125 μm ; final annealed at 640 °C (1180 °F). [Fig. 85](#): grain size is 150 μm ; final annealed at 665 °C (1225 °F). [Fig. 86](#): grain size is 175 μm ; final annealed at 680 °C (1260 °F). [Fig. 87](#): grain size is 200 μm ; final annealed at 705 °C (1300 °F). Etchant 1, [Table 3](#). 75 \times



[graphic]

Fig. 88 Same alloy as [Fig. 80](#), [81](#), [82](#), [83](#), [84](#), [85](#), [86](#), and [87](#). Local (plug-type) dezincification (dark, at specimen surface) consists of a spongy mass of copper that resulted from the selective removal of zinc. Etchant 1, [Table 3](#). 150 \times



[graphic]

Fig. 89 Alloy 28000 (Muntz metal) ingot, as-cast. Structure is dendrites of α phase in a matrix of β phase. Etchant 1, [Table 3](#). 210 \times

[graphic]



Fig. 90 Same as [Fig. 89](#), showing α feathers that formed at β grain boundaries during quenching of the all- β structure. Etchant 1, [Table 3](#). 105 \times

[graphic]



Fig. 91 Same as [Fig. 89](#), hot-rolled plate. Uniform (layer) dezincification. Alpha grains remain in the corroded area (top). Etchant 1, [Table 3](#). 90 \times

[graphic]



Fig. 92 Cu-27.5Zn-1.0Sn alloy tube. Stress-corrosion crack through the wall of the tube, probably caused by mercury or ammonia. Etchant 1, [Table 3](#). 100 \times

[graphic]



Fig. 93 Alloy 44300 (arsenical admiralty) tube, drawn, stress relieved and bent 180°. Transgranular stress-corrosion crack. Etchant 1, [Table 3](#). 200×

[graphic]



Fig. 94 Same alloy as [Fig. 90](#), drawn and annealed tube. Uniform dezincification, with α grains in the corroded area (dark at the surface). Etchant 1, [Table 3](#). 250×

[graphic]



Fig. 95 Alloy 67500 (manganese bronze A) extruded rod. Iron-rich phase (light, outlined) within β phase (smooth etching) and between α and β phases. Etchant 1, [Table 3](#). 875×

[graphic]

A rectangular box containing a micrograph of Alloy 51000. The image area is currently blank, with only the text "[graphic]" at the top left.

Fig. 96 Alloy 51000 (phosphor bronze, 5% A) rod, extruded, cold drawn, and annealed 30 min at 565 °C (1050 °F). Structure consists of recrystallized α grains with annealing twins. Etchant 4, [Table 3](#). 500×

[graphic]

A rectangular box containing a micrograph of Alloy 64700. The image area is currently blank, with only the text "[graphic]" at the top left.

Fig. 97 Alloy 64700 (silicon-nickel bronze), aged 2 h at 480 °C (900 °F) after solution treatment. Alpha grains appear hazy because of unresolved nickel-silicon precipitate. Etchant 4, [Table 3](#). 200×

[graphic]

A rectangular box containing a micrograph of Alloy 64700 at higher magnification. The image area is currently blank, with only the text "[graphic]" at the top left.

Fig. 98 Same as [Fig. 97](#), but at a higher magnification to reveal nickel-silicon precipitate at grain boundaries and within grains. Etchant 4, [Table 3](#). 500×



[graphic]

Fig. 99 Alloy 70600 (copper nickel, 10% Ni), showing the grain-boundary cracks (dark areas) typical of stress-rupture failure. Etchant 4, [Table 3](#). 300×



[graphic]

Fig. 100 Alloy 74500 (nickel silver, 65-10) cold-rolled sheet, 2.5 mm (0.10 in.) thick, annealed at 650 to 700 °C (1200 to 1290 °F). Longitudinal section shows equiaxed crystallized grains of α solid solution containing twin bands. Etchant 20, [Table 3](#). 100×



[graphic]

Fig. 101